Six-Axis Rotor Magnetic Suspension Principle for Permanent Magnet Synchronous Motor with Control of the Positive, Negative and Zero-Sequence Current Components

Gael Messager and Andreas Binder

Institute of Electrical Energy Conversion
Darmstadt University of Technology, Darmstadt, 64283, Germany
gmessager@ew.tu-darmstadt.de, abinder@ew.tu-darmstadt.de

Abstract **─** A novel magnetic levitation principle, applicable for two- and four-pole high-speed permanent magnet synchronous motors, is presented. The drive consists of two half-motors, in which two asymmetric star-connected windings are arranged. An additional active magnetic bearing part is inserted to control the axial displacement. The two coils of the axial magnetic bearing are fed by the zero-sequence current components of the star-connected windings. The proper control of the positive, the negative, and the zero-sequence currents permits to set the torque, the radial levitation forces and the axial levitation force, respectively.

Index Terms **─** Magnetic suspension, permanent magnet synchronous motor, self-bearing motor, symmetrical components.

I. INTRODUCTION

In the past decades, different levitation principles were investigated to achieve rotor suspension with forces of magnetic origin. This paper focuses on a solution with active control of the six degrees of freedom of the rotor, suitable for high-speed drives. Active self-bearing suspension is considered to be an alternative to active magnetic bearings, where the same iron stack is used for the generation of the torque and of the levitation forces [1]. While most self-bearing motors generate only radial suspension forces [1], some unconventional motor designs enable to generate also an axial thrust. A solution is presented in [2], where axial forces are generated by two opposing half-motors with conical air-gap. The axial displacement is controlled actively using a three-point d-current control in each half-motor. In [3], a different approach is proposed, with again two conical half-motors, but here the permanent magnet field is controlled in the synchronous coordinate system. Four conventional windings are required, two for the torque and the axial force, and two for the two radial forces of the two half-motors. Axial flux motor alternatives are proposed in [4] and [5], where the axial thrust results from the difference of the main field on both sides of an axial flux motor. A Lorentz-force based application can be found in [6], where the two counteracting axial thrusts of two conically shaped skewed windings are used to generate a net axial force. A much simpler Lorentz-force based solution is presented in [7]. This latest prototype is composed of two cylindrical half-rotors. Two oppositely skewed windings are brought in two half motors, so that a *q*-current feeding results simultaneously in a torque and an axial thrust. The net torque is produced by a common *q*-current feeding, while the net axial thrust results from an opposite *q*-current feeding. In this paper, an alternative topology is presented, with a thrust bearing as a magnetic active part, fed by two zero-sequence current components from two double star windings. This topology, restricted to two- and four-pole motors, is extended from the motor design presented in [8]. Whereas the previous design [8], requires an additional axial magnetic bearing and the corresponding power electronics, the feeding of the magnetic bearing in the proposed design is achieved through the drive winding itself. As a result, all the terminals are used to generate the torque, the radial and the axial levitation forces simultaneously. In steady-state condition, these components correspond to the positive, the negative and the zero-sequence current components, respectively, in each of the three-phase windings. The first part of the paper describes the different windings in the different active parts, and their feeding. It describes in particular the thrust bearing coils to generate an axial force and their connection to the main windings. The second part focuses on the integration of the zero-sequence current control into the existing control, presented in [8]. It presents a new set of coordinate systems, relevant for the field orientation control. The third part presents an extension of the voltage modulators, which enables to impress a zero-sequence voltage. It is demonstrated, that with simple transformations the determination of the pulse widths to impress the positive and negative sequence voltages is similar to the familiar space vector

Submitted On: October 14, 2016
Accepted On: February 4, 2017

modulation. The determination of the zero-sequence voltage is explained in the fourth part. In particular, the problem of over-modulation is addressed.

II. WINDING CONFIGURATION AND FEEDING

In order to achieve the suspension and speed control of a free rotating body, the six degrees of freedom (DOF) need to be actively controlled. To do so, the torque, the axial force and two sets of two radial forces, on two parallel, but distinct planes, are produced by several electromagnetic actuators. The configuration of the proposed magnetic active parts is represented in Fig. 1.

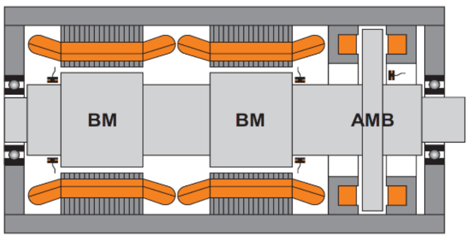

Fig. 1. Schematic representation of the proposed motor with two half permanent magnet synchronous motors (BM) and an active thrust magnetic bearing (AMB).

The proposed drive is composed of two half-motors (BM in Fig. 1), which generate torque and radial levitation forces, and one thrust magnetic bearing part (AMB in Fig. 1), which produces an axial levitation force. To prevent rotor damage in case of levitation control failure, an emergency bearing is present at each rotor end. A play between rotor and bearing inner-ring prevents any mechanical contact during normal operation. Five position sensors and a rotor angle sensor are present to measure the rotor position. Two parallel magnetized two-pole magnets are surface mounted on the rotor. In the stator slots of each half motor two asymmetrical three-phase windings are wound, as shown in Fig. 2. The windings are here represented with a number of slots per pole and phase of q = 1 for clarity. Due to coil short pitching (W/τ_p = 1/2) and an asymmetrical winding arrangement (Fig. 2), the two windings produce not only a fundamental field for the torque, but also a space harmonic of order two (ν = -2) for the radial forces. The expression of the torque (resp. of the radial forces), generated by a differential-mode counter-clockwise rotating current space vector $i_{ccw} = i_{\alpha,1} + \mathrm{j}\, i_{\beta,1}$ (resp. a common-mode clockwise rotating current space vector $i_{cw} = i_{\alpha,-2} + \mathrm{j}\, i_{\beta,-2}$), is detailed in [8]. Additionally, the star points N_A and N_B of the proposed windings (Fig. 2) are interconnected, so it is possible to feed a zero-sequence current $i_{d,0}$ between the two three-phase windings (Fig. 3). This current component is used to generate an axial attraction force. The axial active magnetic bearing is a conventional thrust bearing with differential windings. It is composed of two ring electromagnets with two coils, which are fed according to the differential feeding principle. The outer electromagnet is removable in axial direction to enable the rotor insertion. The two star points N_A and N_B of the two three-phase systems from one half-motor (Fig. 2) are connected to the terminals of one of the two coils (AMB Fig. 1) of the magnetic thrust bearing. The two other star points from the second half-motor winding are connected to the second coil of the magnetic bearing. Two zero-sequence currents $i_{d,0,DE}$ and $i_{d,0,NDE}$ are flowing through the two coils of the magnetic bearing. The amplitudes of the currents $i_{d,0,DE}$ and $i_{d,0,NDE}$ follow the differential feeding Equation (1):

$$\begin{cases} i_{d,0,DE} = i_{0,bias} + \Delta i_0 \\ i_{d,0,NDE} = i_{0,bias} - \Delta i_0 \end{cases} . \qquad (1)$$

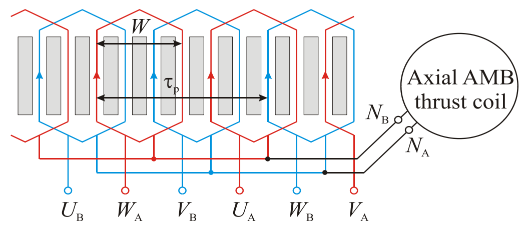

Fig. 2. Winding disposition in one half-motor (e.g., DE BM), connected to a single coil of the thrust bearing (AMB). The thrust coil (on the right) is fed through the interconnected star points N_A, N_B. The winding disposition is identical for the second half-motor.

Whereas the electromagnetic forces, resulting on the thrust disk and generated by the common mode bias current $i_{0,bias}$, are cancelling each other, the differential current Δi_0 produces a net axial force Δf_z. This principle is identical to the principle of differential feeding in active magnetic bearings. The expressions of the phase currents in U_A, V_A, W_A and U_B, V_B, W_B in stationary conditions are shown in (2) and are valid for the drive end (DE) and the non-drive end (NDE) separately. Φ_1 and Φ_2 are the phase angles of the current space vectors i_{ccw} and i_{cw} at the time t = 0. The current space vector i_{ccw} rotates with electrical frequency ω in the positive direction (counter-clockwise), whereas the current space vector i_{cw} rotates with the same electrical frequency ω in the negative direction (clockwise);

$$\boldsymbol{i}_A(t) = \left(i_{U,A}(t),\ i_{V,A}(t),\ i_{W,A}(t)\right)^T = \begin{pmatrix} i_{ccw}\cdot\cos(\omega t+\phi_1)+i_{cw}\cdot\cos(-\omega t+\phi_2)+i_{d,0}/3 \\ i_{ccw}\cdot\cos(\omega t-2\pi/3+\phi_1)+i_{cw}\cdot\cos(-\omega t-2\pi/3+\phi_2)+i_{d,0}/3 \\ i_{ccw}\cdot\cos(\omega t-4\pi/3+\phi_1)+i_{cw}\cdot\cos(-\omega t-4\pi/3+\phi_2)+i_{d,0}/3 \end{pmatrix} \qquad (2)$$

$$\boldsymbol{i}_B(t) = \left(i_{U,B}(t),\ i_{V,B}(t),\ i_{W,B}(t)\right)^T = \begin{pmatrix} i_{ccw}\cdot\cos(\omega t-\pi+\phi_1)+i_{cw}\cdot\cos(-\omega t+\phi_2)-i_{d,0}/3 \\ i_{ccw}\cdot\cos(\omega t+\pi/3+\phi_1)+i_{cw}\cdot\cos(-\omega t-2\pi/3+\phi_2)-i_{d,0}/3 \\ i_{ccw}\cdot\cos(\omega t-\pi/3+\phi_1)+i_{cw}\cdot\cos(-\omega t-4\pi/3+\phi_2)-i_{d,0}/3 \end{pmatrix}$$

The levitation control is identical to the one for drive with active magnetic bearings [1]. It can be realized for example with simple PID controllers that take the displacement position signals as input and calculate the required radial and axial forces to suspend the rotor at the center of the stator.

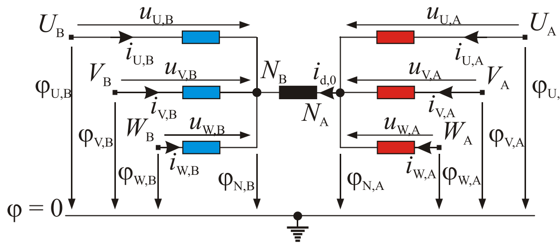

Fig. 3. Schematic representation of the six-phase winding in one half motor (Fig. 2) and definition of the currents and voltage potentials. The second winding in the second half motor is identical.

III. CONTROL STRUCTURE EXTENSION

For independent control of the torque and levitations forces, the six phase currents are transformed into two sets (DE & NDE) of three orthogonal sub-spaces $K_{S,0}$, $K_{dq,1}$, $K_{dq,-2}$. The decomposition is done as follows: The six phase currents are projected on a first stator-based subspace $K_{S,1}$ via (3) to get the differential counter-clockwise components $i_{\alpha,1}$ and $i_{\beta,1}$. It is demonstrated in [8] that these components generate a two-pole magnetic air-gap field. These components are transformed into the synchronous coordinate system $K_{dq,1}$ to control the field weakening and the torque independently. The projection of the phase currents on a second sub-space $K_{S,-2}$ via (3) gives the common-mode clockwise components $i_{\alpha,-2}$ and $i_{\beta,-2}$, which are necessary to produce radial forces. These components are exciting a four-pole air-gap field (harmonic order ν = -2), which interacts with the two-pole rotor permanent magnet field to generate the radial forces [8]. To obtain an independent control of the horizontal and vertical radial forces, these components are transformed into a clockwise rotating coordinate system $K_{dq,-2}$, rotating with the electrical frequency ω. Since the number of pole-pairs of the levitation field (p_2 = 2) is different from the one of the rotor field (p_1 = 1), the levitation field harmonic ν = -2 rotates in stationary condition at a slip s = 0.5 (4). Finally, the projection of the six phase currents on $K_{S,0}$ via (3) gives a single differential zero-sequence current component $i_{d,0}$. Whereas the radial suspension forces and the torque in each half motor are independent from each other, the net axial force results from the difference of the axial forces, generated by the two currents $i_{d,0,DE}$ and $i_{d,0,NDE}$. When these two components are controlled according to (1), the resulting net force Δf_z is directly proportional to Δi_0. The described current projections are factorized according to (3). The control of each current component is done in the sub-spaces $K_{S,0}$, $K_{dq,1}$, $K_{dq,-2}$, for each half motor (DE and NDE in Fig. 1) with simple PI controllers. The voltage outputs are then transformed back to the set of stator coordinate systems $\{K_{S,0}, K_{S,1}, K_{S,-2}\}$ before being sent to the modulators. The speed and position control scheme as well as the linearized model of the proposed drive is identical to the one with active magnetic bearing suspension and is therefore not explained here. An overview of the considered sub-spaces is given in Table 1, with the corresponding space dimension:

$$\begin{pmatrix} i_{\alpha,1} \\ i_{\beta,1} \\ i_{\alpha,-2} \\ i_{\beta,-2} \\ i_{d,0} \end{pmatrix} = \frac{1}{6} \begin{pmatrix} 2 & -1 & -1 & -2 & 1 & 1 \\ 0 & \sqrt{3} & -\sqrt{3} & 0 & -\sqrt{3} & \sqrt{3} \\ 2 & -1 & -1 & 2 & -1 & -1 \\ 0 & \sqrt{3} & -\sqrt{3} & 0 & \sqrt{3} & -\sqrt{3} \\ 3 & 3 & 3 & -3 & -3 & -3 \end{pmatrix} \begin{pmatrix} i_{U,A} \\ i_{V,A} \\ i_{W,A} \\ i_{U,B} \\ i_{V,B} \\ i_{W,B} \end{pmatrix}, \quad (3)$$

$$s = [n_{syn} - (-(n_{syn} / -2))] / n_{syn} = 0.5\,. \quad (4)$$

Table 1: List of the defined sub-spaces

Name	Description	Dim.
$K_{S,0}$	Stator zero-sequence sub-space	1
$K_{dq,1}$	Counter-clockwise synchronous differential component sub-space	2
$K_{dq,-2}$	Clockwise synchronous common-mode component sub-space	2
$K_{S,1}$	Stator counter-clockwise differential component sub-space	2
$K_{S,-2}$	Stator clockwise common-mode component sub-space	2
$K_{S,A}$	($\alpha\beta\gamma$) stator sub-space of winding A	3
$K_{S,B}$	($\alpha\beta\gamma$) stator sub-space of winding B	3

IV. SPACE VECTOR MODULATION EXTENSION

The proposed winding has six phases and five degrees of freedom (DOF). The six phase terminal potentials $\varphi_{U,A}$, $\varphi_{V,A}$, $\varphi_{W,A}$, $\varphi_{U,B}$, $\varphi_{V,B}$, $\varphi_{W,B}$ are impressed by a six phase inverter. It is shown in Fig. 3 that the star-point potentials $\varphi_{N,A}$ and $\varphi_{N,B}$ are not impressed by the inverter, so the 3D SVM is not suitable for this problem. Indeed, the two modulators, necessary to calculate the proper firing instants of the power switches, require a novel pulse width modulation to impress a zero-sequence voltage $u_{d,0}$. Here, a solution is proposed, based on the space vector modulation principle. The pulse pattern of a single six-phase system (Fig. 4) is described by six pulse widths ($t_{0,A}$, $t_{1,A}$, $t_{2,A}$, $t_{0,B}$, $t_{1,B}$ and $t_{2,B}$). The voltage space, covered by this 5D SVM, forms a 5D polytope. In contrast to the common 2D SVM, projections of the reference voltage vectors in 5D voltage spaces are difficult to apprehend. In Fig. 3, the phase voltages $u_{U,A}$, $u_{V,A}$, $u_{W,A}$, can be determined as a function of the phase potentials $\varphi_{U,A}$, $\varphi_{V,A}$, $\varphi_{W,A}$ and the star point potential $\varphi_{N,A}$. Obviously, the two star point potentials $\varphi_{N,A}$ and $\varphi_{N,B}$ are functions of all the six phase potentials $\varphi_{U,A}$, ..., $\varphi_{W,B}$. After projection of the phase voltage vector $\boldsymbol{u}_{\mathbf{A}} = (u_{U,A}, u_{V,A}, u_{W,A})^T$ into the coordinate system $K_{S,A}$ with the Clarke transformation (5), it can be noticed that the components $u_{\alpha,A}$ and $u_{\beta,A}$ of $\boldsymbol{u}_{\mathbf{A}}$, in $K_{S,A}$, are independent of $\varphi_{U,B}$, $\varphi_{V,B}$ and $\varphi_{W,B}$. Doing the same transformation in $K_{S,B}$ with $\boldsymbol{u}_{\mathbf{B}} = (u_{U,B}, u_{V,B}, u_{W,B})^T$, it is possible to split the 5 DOF problem into smaller problems by projection of the stator voltage vector $\boldsymbol{u}_{\mathbf{S}} = (u_{\alpha,1}, u_{\beta,1}, u_{\alpha,-2}, u_{\beta,-2}, u_{d,0})^T$ in $K_{S,A}$ and $K_{S,B}$. The zero-voltage components $u_{0,A}$ and $u_{0,B}$ depend however on all the phase potentials $\varphi_{U,A}$, ..., $\varphi_{W,B}$. While the actual values of $u_{0,A}$ and $u_{0,B}$ are not of interest, the zero-sequence voltage $u_{d,0}$, which drives the zero-sequence current component $i_{d,0}$ in $K_{S,0}$, is given by $u_{d,0} = \varphi_{N,A} - \varphi_{N,B}$. To take advantage of the orthogonality mentioned above, a two-step calculation of the pulse pattern is introduced. First the four pulse widths $t_{1,A}$, $t_{2,A}$, $t_{1,B}$ and $t_{2,B}$ of the active voltage switching states $V_{1,A}$, $V_{2,A}$, $V_{1,B}$ and $V_{2,B}$ are determined to generate solely the counter-clockwise differential voltage space vector components ($u_{\alpha,1}$, $u_{\beta,1}$) and the clockwise common-mode voltage space vector components ($u_{\alpha,-2}$, $u_{\beta,-2}$). To do so, relation (6) is used, followed by two inverse Clarke transformations in A and B. In a second step, the pulse widths $t_{0,A}$, $t_{0,B}$, $t_{7,A}$ and $t_{7,B}$ of the zero-voltage switching states $V_{0,A}$, $V_{0,B}$, $V_{7,A}$ and $V_{7,B}$ are determined to get the required zero-sequence differential voltage component $u_{d,0}$. The general determination of the zero-voltage pulse widths is an underdetermined problem, so that symmetry considerations and polytope boundaries are exploited to find a unique solution. Despite its simplicity, this algorithm is only suited to this particular problem and is not a general solution of the 5D SVM:

$$\begin{pmatrix} u_{\alpha,A} \\ u_{\beta,A} \\ u_{0,A} \end{pmatrix} = \frac{1}{3}\begin{pmatrix} 2 & -1 & -1 \\ 0 & \sqrt{3} & -\sqrt{3} \\ 1 & 1 & 1 \end{pmatrix}\begin{pmatrix} u_{U,A} \\ u_{V,A} \\ u_{W,A} \end{pmatrix} = \frac{1}{3}\begin{pmatrix} 2\varphi_{U,A} - \varphi_{V,A} - \varphi_{W,A} \\ \sqrt{3}\left(\varphi_{V,A} - \varphi_{W,A}\right) \\ \varphi_{U,A} + \varphi_{V,A} + \varphi_{W,A} - 3\varphi_{N,A} \end{pmatrix}, \tag{5}$$

$$\begin{pmatrix} u_{\alpha,A} \\ u_{\beta,A} \\ u_{\alpha,B} \\ u_{\beta,B} \end{pmatrix} = \frac{1}{2}\begin{pmatrix} 1 & 0 & 1 & 0 \\ 0 & 1 & 0 & 1 \\ -1 & 0 & 1 & 0 \\ 0 & -1 & 0 & 1 \end{pmatrix}\begin{pmatrix} u_{\alpha,1} \\ u_{\beta,1} \\ u_{\alpha,-2} \\ u_{\beta,-2} \end{pmatrix}. \tag{6}$$

V. CONTROL OF THE ZERO-SEQUENCE CURRENT

In the proposed scheme, the zero-sequence voltage $u_{d,0}$ is modulated with the difference of pulse width of the zero-voltage switching states $V_{0,A}$, $V_{0,B}$, $V_{7,A}$ and $V_{7,B}$. In order to produce a positive zero-voltage component $u_{d,0}$, the pulse width $t_{7,A}$, of the positive zero-voltage switching state $V_{7,A}$ ("ppp", where all three phase terminals are switched to U_{dc}) in the three-phase system A is increased, while the pulse width $t_{7,B}$ of the positive zero-voltage switching state $V_{7,B}$ in the three-phase system B is reduced (Fig. 4). The variation of the zero-of $u_{d,0}$ over a switching period T_{sw}, becomes positive. An illustration of asymmetrical pulse patterns is given in Fig. 4. The determination of the four zero-voltage pulse widths $t_{0,A}$, $t_{0,B}$, $t_{7,A}$ and $t_{7,B}$ is formulated as (7), (8) and (9):

$$\left(t_{0,A}, t_{7,A}, t_{0,B}, t_{7,B}\right) \in \mathbb{R}^4_{\geq 0}, \tag{7}$$

$$t_{Z,i} = t_{0,i} + t_{7,i} = T_{sw} - t_{1,i} - t_{2,i} \geq 0 \quad i = \text{A,B}, \tag{8}$$

$$\frac{k_{eq}}{T_{sw}} \cdot \int_0^{T_{sw}} \sum_{i=U,V,W} \left(\varphi_{i,A}(t) - \varphi_{i,B}(t)\right) \cdot dt = u_{d,0}(t). \tag{9}$$

Whereas the two first conditions (7) and (8) are very simple to compute, the third condition (9) requires those machine parameters, which are relevant for the zero-sequence components. A simplified equivalent circuit of the zero-sequence system is proposed in Fig. 5, which considers due to the high switching frequency only the inductances, which are limiting the zero-sequence current $i_{d,0}$. The zero-sequence current $i_{d,0}$ magnetizes the air-gap of the two half-motors BM (Fig. 1) with a field space harmonic of order three ($\nu = 3$). It magnetizes additional regions in the slots and winding overhangs as well. The equivalent leakage inductance is named $L_{\sigma,0,BM}$ for A and B. It also magnetizes the leakage inductance of the magnetic bearing AMB (Fig. 1) itself, which is called $L_{\sigma,AMB}$. Finally it magnetizes the magnet bearing air-gap region of interest with a magnetizing inductance $L_{h,AMB}$. Integrating the left side of (9), it can be shown that the third condition is equivalent to (10), where the coefficient k_{eq} characterizes the equivalent voltage divider of the circuit (Fig. 5) according to (11):

$$\frac{k_{eq}}{T_{sw}} \cdot \int_0^{T_{sw}} \sum_{i=U,V,W} \left(\varphi_{i,A}(t) - \varphi_{i,B}(t)\right) \cdot dt = u_{d,0}(t), \tag{10}$$

$$k_{eq} = \frac{L_{h,AMB} + L_{\sigma,AMB}}{3 \cdot (L_{h,AMB} + L_{\sigma,AMB}) + 2\, L_{0,BM}}. \tag{11}$$

In order to obtain a single formulation of the solution, the pulse width t_1 is defined so that t_1 corresponds to the first active voltage state "pnn", where one of the three phases is at the DC link voltage U_{dc}, while the two others are switched to ground potential. The pulse width t_2 corresponds to the second active voltage state "ppn", where two of the three phases are switched to U_{dc}, while the remaining one is switched to ground potential. Following this convention, the third condition is reformulated as (12). Finally the solution ($t_{0,A}$, $t_{0,B}$, $t_{7,A}$, $t_{7,B}$) of the problem is given by the intersection of three hyper-surfaces in $\mathbb{R}^4_{\geq 0}$, defined by (8) and (12). As a consequence, the solution can be underdetermined, or a single point, or there can be no solution at all. The underdetermined case occurs, when the reference zero-sequence voltage $u_{d,0}$ is small enough, and the inverter has enough voltage reserve, (i.e., when the modulated active voltage vectors $(u_{\alpha,A}, u_{\beta,A})^T$ and $(u_{\alpha,B}, u_{\beta,B})^T$ in windings A and B are below the maximal admissible voltage vector amplitude). In the underdetermined case, the additional constraint (13) is proposed where the pulse widths $t_{Z,A}$ and $t_{Z,B}$ are defined in (8) and the pulse width $t_{Z,MB}$ is defined in (12):

$$\begin{aligned} t_{Z,MB} &= t_{7,A} - t_{0,A} - t_{7,B} + t_{0,B} \\ &= \frac{2T_{sw}u_0}{3k_{eq}U_{dc}} - \left[\frac{t_{2,A}-t_{1,A}}{3} - \frac{t_{2,B}-t_{1,B}}{3}\right], \end{aligned} \tag{12}$$

$$t_{7,A} - t_{0,A} = \frac{t_{Z,A}t_{Z,MB}}{t_{Z,A}+t_{Z,B}} \Leftrightarrow t_{7,B} - t_{0,B} = -\frac{t_{Z,B}t_{Z,MB}}{t_{Z,A}+t_{Z,B}}, \tag{13}$$

$$(t_{0,i}, t_{7,i}) = (0, t_{z,i}) \text{ or } (t_{z,i}, 0),\ i = \text{A,B}, \tag{14}$$

$$\begin{aligned} t_{0,A} &= \frac{1}{2}\left(t_{Z,A} - \frac{t_{Z,B}}{t_{Z,A}+t_{Z,B}}t_{Z,MB}\right), \\ t_{0,B} &= \frac{1}{2}\left(t_{Z,B} - \frac{t_{Z,A}}{t_{Z,A}+t_{Z,B}}t_{Z,MB}\right), \\ t_{7,A} &= \frac{1}{2}\left(t_{Z,A} + \frac{t_{Z,B}}{t_{Z,A}+t_{Z,B}}t_{Z,MB}\right), \\ t_{7,B} &= \frac{1}{2}\left(t_{Z,B} + \frac{t_{Z,A}}{t_{Z,A}+t_{Z,B}}t_{Z,MB}\right). \end{aligned} \tag{15}$$

This condition (13) is chosen to get a continuous transition of the solutions ($t_{0,A}$, $t_{0,B}$, $t_{7,A}$, $t_{7,B}$) when $t_{Z,A} = 0$ or $t_{Z,B} = 0$ in (8) (i.e., when one modulated active vector $(u_{\alpha,A}, u_{\beta,A})^T$ or $(u_{\alpha,B}, u_{\beta,B})^T$ reaches the maximal admissible voltage vector amplitude). The Equations (8), (12) and (13) are reformulated in a matrix form and the explicit solution (15) is obtained by inversion of the matrix. When no solution is possible (i.e., when $t_{Z,A} < 0$ or $t_{Z,B} < 0$ or $t_{Z,A} + t_{Z,B} = 0$), the reference voltage amplitude is too high, and/or the inverter has not enough voltage reserve. In this case, the modulator algorithm provides the maximum voltage amplitude available by following the over-modulation (14). For proper operation of the levitated drive however, field weakening operation should be considered. The expression of k_{eq} (11) shows that the magnetizing inductance of the magnetic bearing $L_{h,AMB}$ should be intentionally designed to be big, and the other leakage inductances should be low, to prevent an inverter over-sizing. The two-step calculation is done as follows: During a control period T_{sw}, after all the current control calculations are completed, the reference voltage vector $\boldsymbol{u} = (u_{d,1}, u_{q,1}, u_{d,-2}, u_{q,-2}, u_{d,0})^T$ in $\{K_{S,0}, K_{dq,1}, K_{dq,-2}\}$ is transformed into the stator sub-spaces $\{K_{S,0}, K_{S,1}, K_{S,-2}\}$ to obtain $\boldsymbol{u}_S = (u_{\alpha,1}, u_{\beta,1}, u_{\alpha,-2}, u_{\beta,-2}, u_{d,0})^T$. The vector components $u_{\alpha,1}$, $u_{\beta,1}$, $u_{\alpha,-2}$ and $u_{\beta,-2}$ are then projected on the α-β planes A and B with (6). Thanks to the orthogonality properties explained above, the calculation of the pulse widths $t_{1,A}$ and $t_{2,A}$ (resp. $t_{1,B}$ and $t_{2,B}$, Fig. 4) to modulate solely the voltage components $u_{\alpha,A}$, $u_{\beta,A}$ (resp. $u_{\alpha,B}$, $u_{\beta,B}$) is the same as for the conventional 2 DOF SVM. In a second step, the pulse widths $t_{0,A}$ and $t_{7,A}$ (resp. $t_{0,B}$ and $t_{7,B}$, Fig. 4) of the two zero-voltage switching states $V_{0,A}$ and $V_{7,A}$ (resp. $V_{0,B}$ and $V_{7,B}$) are determined with (15). When there is no solution, (14) is used instead to insure maximum amplitude of the zero-sequence voltage $u_{d,0}$.

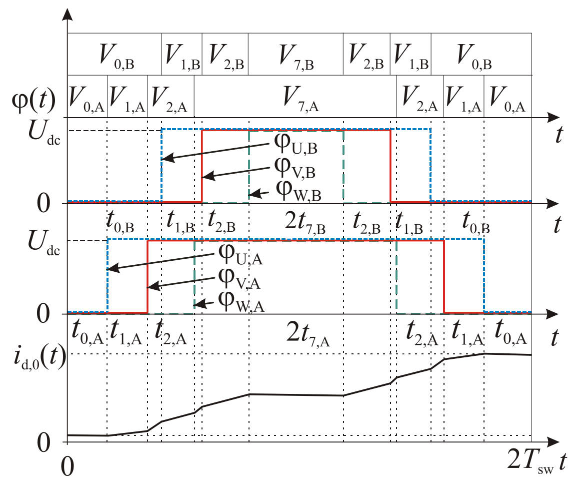

Fig. 4. Example of an asymmetrical pulse pattern for a six-phase system U_A, V_A, W_A, U_B, V_B, W_B (e.g., DE BM) to produce a positive zero-voltage component and two equal active voltage space vectors $(u_{\alpha,A}, u_{\beta,A})^T = (u_{\alpha,B}, u_{\beta,B})^T$. The pulse width of the positive zero-voltage switching state V_7 is larger in the winding A than in the winding B. Hence, the resulting zero-sequence current $i_{d,0}$ increases.

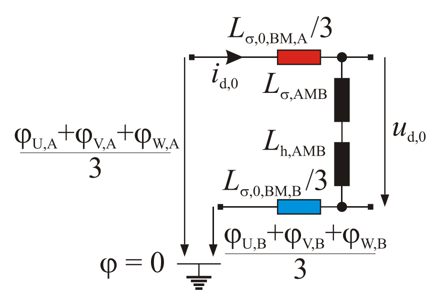

Fig. 5. Simplified inductive equivalent circuit of the zero-sequence component. The two half motors (BM: DE & NDE) are described by the two zero-sequence winding leakage inductances $L_{\sigma,0,BM}$. The axial magnetic bearing is described by a winding leakage inductance $L_{\sigma,AMB}$ and a magnetizing inductance $L_{h,AMB}$.

VI. CONCLUSION

A new six degree of freedom magnetic suspension system is presented. It consists of sets of antisymmetric three phase windings interconnected at the star points. The control of such windings requires an extension of the field orientation control to transform the phase currents into three independent sub-spaces $K_{S,0}$, $K_{dq,1}$, $K_{dq,-2}$. A two-step calculation is presented to determine the SVM pulse pattern, which is necessary for the control of the zero-sequence current component $i_{d,0}$.

REFERENCES

[1] A. Chiba, T. Fukao, O. Ichikawa, M. Oshima, M. Takemoto, and D. G. Dorrell, *Magnetic Bearings and Bearingless Drives*. Oxford: Elsevier Linacre House, 2005.

[2] P. E. Kascak, "*Fully levitated rotor magnetically suspended by two pole-pair separated conical motors*," Ph.D. Thesis, Case Western Reserve University, Cleveland (OH, USA), 2010.

[3] G. Munteanu, A. Binder, and S. Dewenter, "Five-axis magnetic suspension with two conical air gap bearingless PM synchronous half-motors," in *Proceedings of the International Symposium on Power Electronics, Electrical Drives, Automation and Motion (SPEEDAM), 2012*, pp. 1246-1251, Sorrento, Italy, 20-22 June 2012.

[4] J. Asama, Y. Hamasaki, T. Oiwa, and A. Chiba, "Proposal and analysis of a novel single-drive bearingless motor," in *IEEE Transactions on Industrial Electronics*, vol. 60, no. 1, pp. 129-138, Jan. 2013.

[5] Q. D. Nguyen and S. Ueno, "Analysis and control of non-salient permanent magnet axial gap self-bearing motor," in *IEEE Transactions on Industrial Electronics*, vol. 58, no. 7, pp. 2644-2652, July 2011.

[6] J. Abrahamsson, J. Ogren, and M. Hedlund, "A fully levitated cone-shaped Lorentz-type self-bearing machine with skewed windings," in *IEEE Transactions on Magnetics*, vol. 50, no. 9, pp. 1-9, Sept. 2014.

[7] G. Wu, X. Wang, Q. Ding, and T. Ni, "Design and analysis of a novel axial actively regulated slotless skew winding bearingless motor," in *IEEE International Conference on Mechatronics and Automation (ICMA), 2015*, Beijing, China, pp. 1864-1869, 2-5 Aug. 2015.

[8] G. Messager and A. Binder, "Analytical comparison of conventional and modified winding for high speed bearingless permanent magnet synchronous motor applications", in *International Conference on Optimization of Electrical and Electronic Equipment (OPTIM), 2014*, Brasov, Romania, pp. 330-337, 22-24 May 2014.

Gael Messager was born in Cannes La Bocca in France. He received the M. degree in Electrical Engineering from the Technical University of Darmstadt, Darmstadt, Germany, in 2012 where he is currently working toward the Ph.D. degree. His current research interests include design and control of high speed bearingless motors.

Andreas Binder Senior Member IEEE, Member VDE, IET, VDI, EPE, received the degrees Dipl.-Ing. (diploma) and Dr. Techn. (Ph.D.) for Electrical Engineering from the University of Technology, Vienna/ Austria, in 1981 and 1988, respect-ively. From 1981 to 1983 he worked at ELIN-Union AG, Vienna, on large synchronous generator design. From 1983 to 1989 he joined the Institute of Electrical Machines and Drives, Technical University, Vienna, as Researcher. From 1989 to 1997 he rejoined industry, leading groups for developing DC and inverter-fed AC motors and drives, at Siemens AG, Bad Neustadt and Erlangen, Germany. Since 1994 he is Lecturer (habilitation) at University of Technology, Vienna/Austria, and received in 1997 the ETG-Literature Award of the German Assoc. of Electrical Engineers, VDE. Since October 1997, he is Head of the Institute of Electrical Energy Conversion, Darmstadt University of Technology, as a Full Professor, being responsible for teaching and research for electrical machines, drives and railway systems. He is the author or co-author of more than 280 scientific publications and two books and holds several patents. He received Dr. h.c. from University of Technology Bucharest in 2007 and is the recipient of the Medal of Honour of the ETG/VDE 2009 for outstanding contributions at VDE.